JOURNAL OF CATALYSIS **175,** 7–15 (1998)
ARTICLE NO. CA981972

Selective Catalytic Reduction of Nitric Oxide by *n*-Decane on Cu/Sulfated-Zirconia Catalysts in Oxygen Rich Atmosphere

Effect of Sulfur and Copper Contents

G. Delahay,[1] E. Ensuque, B. Coq, and F. Figuéras[2]

Laboratoire de Matériaux Catalytiques et Catalyse en Chimie Organique, UMR 5618 CNRS, ENSCM,
8 rue de l'Ecole Normale, 34296 Montpellier Cedex 5, France
E-mail: delahay@cit.enscm.fr

Received May 22, 1997; revised November 6, 1997; accepted November 10, 1997

The effect of sulfur and copper contents on the activity of Cu/sulfated-zirconia (SZ) catalysts, in the selective reduction of NO by *n*-decane, were investigated in the 298–723 K temperature range. ZrO_2 and SZ solids exhibited no activity below 773 K. Cu/ZrO_2 is active and selective at low temperature ($<$600 K) but oxidises selectively NO to NO_2 at higher temperatures. By contrast, whatever the temperature, a 100% selectivity to N_2 is obtained with Cu/SZ catalysts. The highest activity is reached with the catalyst containing the highest number of acid sites which corresponds to a sulfur content close to the amount required to form a sulfate monolayer. Acidity plays a significant role only at temperatures above 600 K, where it is concluded that a bifunctional mechanism governs the reduction of NO to N_2. © 1998 Academic Press

Key Words: **NO_x reduction; nitric oxide; sulfated zirconia; copper.**

1. INTRODUCTION

The selective catalytic reduction (SCR) of NO to N_2 by hydrocarbons in the presence of excess O_2 has been extensively studied as a potential process in NO_x emission control for Diesel and lean-burn engines. The mechanism of this process is complex and depends on the catalyst (1), the type of hydrocarbon (2), and the reaction conditions (3). Nevertheless, various reaction schemes have been proposed: (i) a redox mechanism involving Cu^I, generated through reduction of Cu^{II} by hydrocarbon (4), (ii) a bifunctional mechanism where NO is oxidised first to NO_2 on the metal oxide, or cationic sites, and then NO_2 would react with an adsorbed hydrocarbon activated by the acid function (5, 6), and (iii) a bifunctional mechanism where hydrocarbons are converted to some intermediates interacting then with NO_x (7, 8).

We recently showed (9), in the SCR of NO by *n*-decane over Cu/ZrO_2, that N_2 was selectively formed at reaction temperature below 573 K (9). In contrast, NO_2 was the main product when the temperature exceeded 673 K. Very interestingly, when the Cu/ZrO_2 catalysts were promoted by sulfate, the conversion of NO by *n*-decane became selective to N_2 whatever the reaction temperature up to 773 K. This effect has been attributed to the increase of acidity and/or to strong interaction between copper and sulfate species. The promoting effect of the acidity on the rate and the selectivity of SCR of NO has been underlined by several authors (10–14). In particular, Loughran and Resasco (14) have shown that sulfated zirconia (SZ) was the most effective material to promote, in mechanical mixtures, the activity of Pd/SiO_2 in SCR of NO by methane. In the same way, a promoting effect of SZ was reported by Delahay *et al.* (10) and by Figuéras *et al.* (11) in the SCR of NO on copper manganite and on titania or zirconia supported copper catalysts, respectively. Therefore, the acid site density and/or acid strength may play an important role. On the other hand, solid acids exhibit some activity in SCR of NO, as shown for hydrogen exchanged zeolites (15–19) and for some sulfate promoted metal oxides (20, 21). However, their activity remains much lower than that of bifunctional catalysts, containing a transition metal.

It thus appeared interesting to investigate the effect of sulfur and copper contents in Cu/SZ catalysts, in order to modify their acidity and redox properties respectively, on the SCR of NO by *n*-decane under O_2 rich atmosphere.

2. EXPERIMENTAL

2.1. *Catalyst Preparation*

Zirconium hydroxide was obtained by adding dropwise concentrated NH_4OH solution to a $ZrOCl_2 \cdot 8H_2O$ (Fluka) solution at a constant $pH = 10$. The precipitate was filtered,

---

[1] Author to whom correspondence should be sent.

[2] Present address: Institut de Recherches sur la Catalyse du CNRS, 2 Avenue A. Einstein, 69626 Villeurbanne Cedex, France.

0021-9517/98 $25.00

repeatedly washed with distilled water until no chloride was detected, and dried overnight at 393 K. The SZ samples were prepared by contacting an adequate amount of dried $Zr(OH)_4$ with 250 cm^3 of a H_2SO_4 solution; the slurry was then stirred for 6 h. After filtering, the solid was dried overnight at 393 K. In order to prevent the modification of sulfur content of SZ by deposition of Cu salt in aqueous medium, a dedicated procedure, previously described by Boitiaux *et al.* (22) for preparing well dispersed noble metal supported catalysts, was used to introduce Cu on the supports. Cu catalysts were thus obtained by contacting for 6 h, 3 g of the support (ZrO_2 or SZ), dried overnight at 473 K under He, with an adequate amount of copper acetylacetonate (Janssen) in 200 cm^3 acetylacetone solution (Prolabo). After filtration, the powder was dried at 393 K for 3 h, then calcined under air at 773 K for 3 h. The amounts of sulfur and copper were varied from 1 to 8 wt%. The labelling of the sample, e.g. Cu(3)/SZ(5.3), means that this sample contains 3 wt% Cu and 5.3 wt% S.

The catalytic properties of a Cu/MFI (1.6 wt% Cu, 80% nominal exchange level, Si/Al = 27) supplied by IFP were evaluated for a purpose of comparison. This sample was proved to be very efficient in the SCR of NO by propene and propane (5).

2.2. Catalyst Characterisation

The catalysts were characterised by chemical analysis (Laboratoire d'analyse du CNRS, Vernaison, France), N_2 sorption at 77 K (Micromeritics ASAP 2000), X-ray diffraction (CGR Theta 60 instrument using CuKα monochromated radiation), temperature programmed desorption of acetonitrile (TPD), temperature programmed reduction by H_2 (TPR) and temperature programmed oxidation by oxygen (TPO), and diffuse reflectance UV-visible spectroscopy (Perkin Elmer). The catalytic behaviour of the sample was evaluated for the SCR of NO by *n*-decane in a flow reactor operating at atmospheric pressure.

The acid properties of the samples were evaluated by TPD of CH_3CN using the procedure reported by Figuéras *et al.* (23). For CH_3CN TPD experiments, an aliquot of the catalyst ($\approx$0.100 g) was reactivated *in situ* at 673 K for 1 h in air. After saturation of the sample with CH_3CN at room temperature, the physisorbed CH_3CN was removed by outgassing under N_2 at 363 K. The CH_3CN desorption is then started in N_2 flow (50 cm^3 min^{-1}) from 363 to 823 K at 6 K min^{-1}. The identification of CH_3CN released in the outflowing gas was performed by sampling on line every minute to a gas chromatograph.

The reducibility of copper species was determined by TPR as described elsewhere (24). About 0.085 g of the sample was placed in a quartz reactor and activated at 673 K for 1 h in air (ramp: 5 K min^{-1}). After flushing with high purity He flow, the reactor was cooled down to room temperature. The TPR experiments were carried out using H_2/Ar gas (3/97, vol/vol, purity of both gases >99.995%). The linear temperature program was then started from 293 to 873 K (ramp: 5 K min^{-1}, flow: 20 cm^3 min^{-1}). The experimental set up of TPO was similar with that used for TPR experiments (O_2/He: 3/97, vol/vol, and purity of both gases >99.995%). The following treatment cycle is then applied to the sample: (1) TPR up to 650 K, then (2) TPO up to 650 K, and (3) TPR up to 1173 K.

The nature of Cu species, in Cu/SZ catalysts, was identified by UV-visible spectroscopy and electron spin resonance (ESR) experiments. Diffuse reflectance spectra of the catalysts in the UV-Vis region were recorded at room temperature with a Perkin Elmer UV/Vis Lambda 14 spectrophotometer. The measured reflectance was converted to the corresponding Kubelka–Munk function (KM function) with the aid of a personal computer using an applied program, and was plotted versus the wavelength (in nm). ESR spectrum was obtained at room temperature on a Brüker ER 200D-SRC X-band spectrometer with 100 kHz modulation.

2.3. Catalytic Tests

The SCR of NO by *n*-decane was performed in a flow reactor operating at atmospheric pressure. An aliquot ($\approx$0.050 g) of the powdered catalyst was placed in a reactor and activated *in situ* at 673 K for 1 h in air. After flushing He, the reactor was cooled down to room temperature. The reaction was performed using a gas mixture containing 0.1 vol% NO (purity >99.995%), 0.03 vol% *n*-decane (purity >99.5%) and 9 vol% O_2 (purity >99.995%), the balance with helium. The flow rate was 60 cm^3 min^{-1} (space velocity: 70,000 h^{-1}) and the temperature was varied from 298 to 750 K (ramp: 5 K min^{-1}). The composition of the effluents was monitored continuously by sampling on line to a quadrupole mass spectrometer Balzers QMS 421 equipped with a Faraday detector (0–200 amu) and following the masses 28, 30, 44, 46, and 57. N_2 and CO formations were discriminated by analysing the products with a gas chromatograph (Varian) equipped with a katharometer and a 13X molecular sieve column.

3. RESULTS

3.1. Main Characteristics of the Catalysts: XRD Data and Specific Surface Areas

The characteristic patterns of the tetragonal and monoclinic phases were observed for ZrO_2 (Table 1). Upon addition of 1.0% sulfur, only the tetragonal phase remains and the solid SZ(5.3) was found to be amorphous. This delay of zirconia crystallisation upon sulfate addition is well documented (25) and is also correlated with an increase of the specific surface area till 3.5 wt% S (Table 1), as

TABLE 1

Some Physico–Chemical Characteristics of the Samples

Catalysts	Structure	BET surface area ($m^2\ g^{-1}$)	NO/Cu[a] (mol/mol)
$Zr(OH)_4$	Amorph[b]	290	/
ZrO_2	Tetr + mon[c]	134	/
SZ(1.0)	Tetr	182	/
SZ(1.4)	Tetr	187	/
SZ(2.5)	Tetr	207	/
SZ(3.5)	Tetr	205	/
SZ(5.3)	Amorph	160	/
Cu(3.7)/ZrO_2	Tetr + mon	136	0.42
Cu(3.0)/SZ(1.0)	Tetr	174	0.59
Cu(3.0)/SZ(1.4)	Tetr	163	0.55
Cu(4.0)/SZ(2.5)	Amorph	230	0.34
Cu(3.9)/SZ(3.5)	Amorph	222	0.26
Cu(3.0)/SZ(5.3)	Amorph	158	0.15
Cu(0.8)/SZ(3.5)	Amorph	215	0.57
Cu(3.2)/SZ(3.5)	Amorph	222	0.29
Cu(7.9)/SZ(3.5)	Tetr	147	0.08

[a] Ref. (45).

[b] Amorph = amorphous.

[c] Tetr = tetragonal; mon = monoclinic.

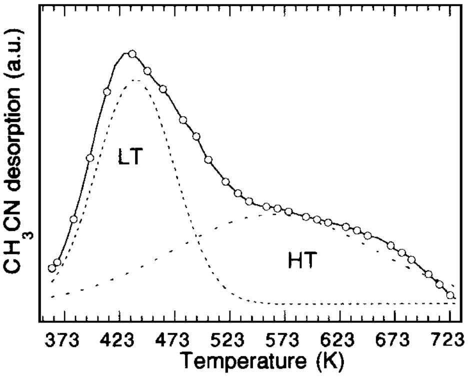

FIG. 1. TPD profile of CH_3CN; SZ(2.5). Conditions: N_2 flow rate = 50 $cm^3\ min^{-1}$; amount of catalyst = 0.100 g; heating rate = 6 K min^{-1}.

previously reported (26, 27). At higher sulfate content, S_{BET} decreased, very likely due to a restricted access to the porosity by pore blockage (28). The specific surface area reaches a maximum of ca 220–230 $m^2\ g^{-1}$ at a sulfur content of ca 2.5–3.5%. After addition of up to 3–4 wt% Cu to ZrO_2 or SZ, textural properties were little affected since S_{BET} were only modified by ±10%. However, a high Cu content (7.9 wt%) induces a 36% decrease of S_{BET} likely due to large CuO aggregates which limit the access of porosity.

3.2. *Study of the Acidity*

Acetonitrile is an appropriate probe to characterize the acid/base properties of the solids (29). CH_3CN interacts, through the lone pair of the N atom, with both Bröensted and Lewis sites, and has been thus used to probe the acidity in zeolites (30, 31) and SZ (23, 31).

After saturation of SZ with CH_3CN at room temperature and evacuation of weakly adsorbed species at 363 K, the desorption of CH_3CN from SZ and Cu/SZ catalysts shows merely two peaks at around 400–420 K (LT) and 550–600 K (HT) (Fig. 1). The total amount of CH_3CN desorbed increases up to a sulfur content of 3.5% and then decreases (Table 2). The respective CH_3CN amounts desorbing under the LT and HT peaks follow the same behaviour, and culminated for a S content of 3.5%. One may discuss about the exact nature of sulfur species occurring at the surface of zirconia, mono- and polydendate sulfates, as well as polymeric sulfates were proposed (32–35). However, assuming that a "monosulfate species" occupies 2.5 nm^2, a fairly nice correlation between the activity in *n*-butane isomerisation and the sulfur content was first proposed by Nascimento *et al.* (27). The maximum activity after calcination at various temperatures was always reached for a final S content corresponding to a coverage of zirconia surface by a theoretical monolayer of sulfate, i.e. $21 \times 10^{-5}\ g_s\ m^{-2}$. We have also found the same behaviour for SZ prepared by a one-step sol-gel synthesis (28). For SZ(3.5) and Cu/SZ(3.5) samples, which contains 3.5 wt% and exhibit S_{BET} of ca 210–220 $m^2\ g^{-1}$, the sulfur species density is about 16–$17 \times 10^{-5}\ g_s\ m^{-2}$, a value close to a hypothetical sulfate monolayer.

The deposition of copper on SZ(3.5) modifies the acidity of the support (Table 2). The amount of weak acid sites is

TABLE 2

Quantitative Analysis of the TPD of Acetonitrile, the TPR by H_2, and the TPO by O_2

	Amount of CH_3CN desorbed ($\mu mol\ m^{-2}$)			TPR by H_2		TPO by O_2	
Catalysts	Total	Under LT	Under HT	T_m[a] (K)	H_2/Cu (mol/mol)	T_{m1}[b] (K)	T_{m2}[b] (K)
SZ(1.0)	1.33	0.67	0.66	—	/	/	/
SZ(1.4)	1.50	0.76	0.74	/	/	/	/
SZ(2.5)	2.00	0.90	1.10	/	/	/	/
SZ(3.5)	2.24	1.10	1.14	/	/	/	/
SZ(5.3)	1.72	1.10	0.62	/	/	/	/
Cu(3.7)/ZrO_2	0.93	0.52	0.41	409	1.00	371	465
Cu(3.0)/SZ(1.0)	0.95	0.69	0.26	491	0.91	379	491
Cu(3.0)/SZ(1.4)	1.17	0.78	0.39	489	0.84	379	489
Cu(4.0)/SZ(2.5)	1.74	1.06	0.68	540	0.95	379	507
Cu(3.9)/SZ(3.5)	2.13	1.25	0.88	563	1.10	388	525
Cu(3.0)/SZ(5.3)	1.60	1.20	0.40	599	0.90	391	533
Cu(0.8)/SZ(3.5)	2.39	1.43	0.96	/	/	/	/
Cu(3.2)/SZ(3.5)	2.00	1.15	0.85	579	0.86	391	525
Cu(7.9)/SZ(3.5)	2.05	1.62	0.43	562	1.00	410	541

[a] Temperature of faster reduction rate.

[b] Temperatures of faster oxidation rate for the first and second peaks.

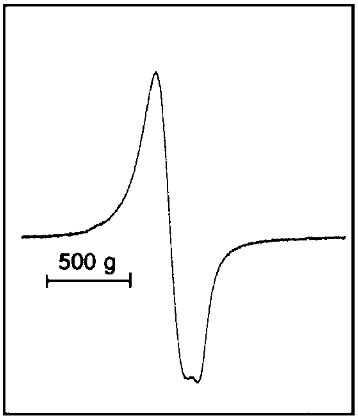

FIG. 2. ESR spectrum of Cu(3.9)SZ(3.5).

slightly higher (a small increase of CH_3CN desorbing at low temperature), at the expense of the strong acid sites. That could reflect that Cu species mainly interact with strong acid sites. However, Cu/SZ(3.5) catalyst always exhibits the greatest number of both weak and strong acid sites. On the other hand, the HT peak of CH_3CN desorption from Cu/ZrO_2 is mainly due to the interaction of CH_3CN with basic sites of ZrO_2 which are inhibited upon the first adsorption of sulfate.

3.3. Nature and Redox Properties of Cu Species

On zirconia-supported Cu catalysts, no diffraction line for CuO phase was detected. On the other hand, the absence of a hyperfine structure in the ESR spectrum of Cu(3.9)SZ(3.5) (Fig. 2) allows us to rule out the presence of isolated Cu^{2+} species. The spectrum is rather characteristic of a loosely ordered copper oxide phase, in agreement with the absence of an XRD pattern.

The UV-visible spectra for Cu/SZ at various sulfate and Cu contents are shown in Figs. 3 and 4, respectively. In the presence of copper, two additional absorption bands are observed in the regions 750–800 and 250–320 nm. The absorption band at 600–900 nm is generally assigned to d–d transitions of Cu^{II} situated in an octahedral environment (36–38). For instance isolated Cu^{2+} species in hydrated Y zeolite exhibit an absorption band above 800 nm while in dehydrated Y zeolite the band is shifted to 960 nm (36). On the other hand, bulk CuO aggregates show an absorption band around 750–800 nm (37, 38). The absorption band at 250–310 nm is attributed to the $Cu^{2+} \leftarrow O^{2-}$ charge transfer. When the sulfur content increases, or copper content decreases, the band at 300 nm is slightly shifted to a lower wavelength and becomes broader. Moreover, the intensity ratio $I_{(205\text{–}300)}/I_{(750\text{–}800)}$ increases with the copper content, but decreases with the sulfur content. On the other hand, no shift of the band at 750–800 nm is observed in both cases.

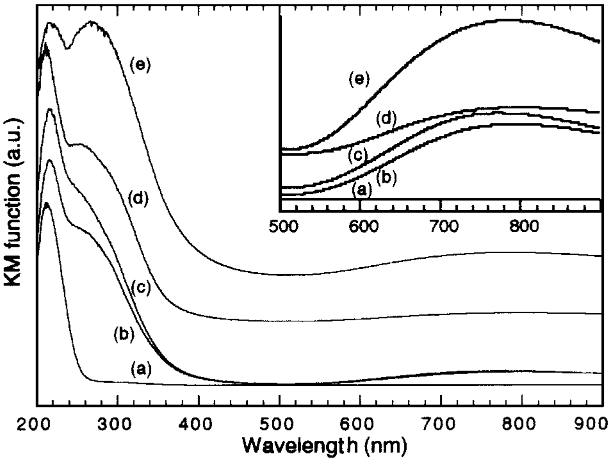

FIG. 3. UV-Visible spectra of: (a) ZS(3.5); (b) Cu(3.0)SZ(1.0); (c) Cu(3.9)SZ(3.5); (d) Cu(3.0)SZ(5.3); and (e) Cu(3.7)ZrO_2.

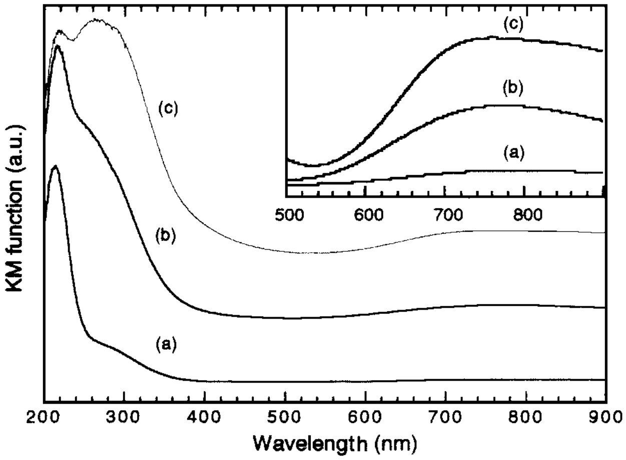

FIG. 4. UV-Visible spectra of: (a)Cu(0.8)SZ(3.5); (b) Cu(3.2) SZ(3.5); and (c) Cu(7.9)SZ(3.5).

When applied to the study of a supported metal catalyst, TPR/TPO experiments provide information about the redox properties of the active species, and the extent of metal–support interactions. Under the TPR conditions we used, ZrO_2 did not show any reduction peak below 900 K and decomposition, with some reduction, of sulfate species in SZ started at around 773 K with a peak maximum in the 823–873 K range. The reduction profile of copper-containing samples shows a unique peak of H_2 consumption below 650 K (Figs. 5 and 6) which is tentatively attributed to reduction of Cu species. Moreover, the presence of Cu induced a temperature shift, by 100–130 K to lower values, of the reduction of sulfate species, which started at ca 630 K. TPR of Cu(3.9)/SZ(3.5) followed by mass spectroscopy has shown that evolution of SO_2, with some H_2S due to sulfate reduction occurs above 630 K. The hydrogen consumption under the lower temperature peak at ca 560 K was only correlated with an H_2O evolution. UV-visible spectroscopy and TPR experiment are thus fully consistent for the reduction of CuO to Cu^0 aggregates occurring under the low

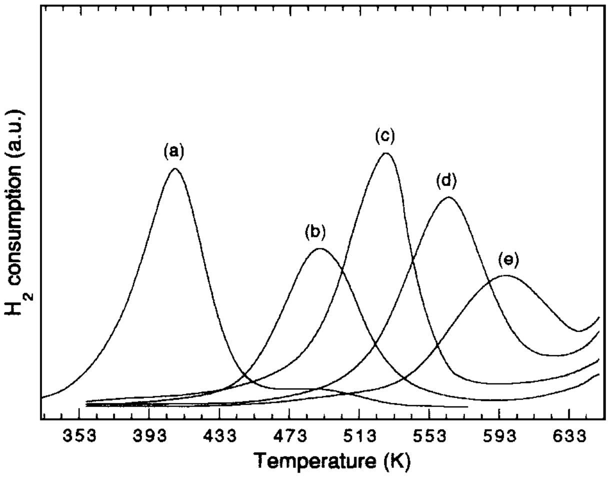

FIG. 5. TPR profiles of: (a) Cu(3.7)ZrO_2; (b) Cu(3.0)SZ(1.4); (c) Cu(4.0): SZ(2.5); (d) Cu(3.9)SZ(3.5); and (e) Cu(3.0)SZ(5.3). Conditions: H_2/Ar: 3/97 (vol/vol); flow rate = 20 cm^3 min^{-1}; amount of catalyst = 0.085 g; heating rate = 5 K min^{-1}.

temperature peak of TPR profiles (Figs. 5 and 6). A similar shift to lower temperature of sulfated decomposition and reduction was observed in the TPR of SZ-supported Ni and Pt catalysts (39–41).

As mentioned above, the TPR profile of CuO/ZrO_2 exhibits a single peak with a maximum at 409 K (Fig. 5). The facile reduction of CuO/ZrO_2 is worth noting. It has been previously shown that the reduction temperature of CuO/SiO_2 decreases from 570 to 500 K when the dispersion of CuO increases (42). However, the very low reduction temperature observed for CuO/ZrO_2 (409 K) cannot be accounted for only a dispersion effect, but also by some kind of $CuO-ZrO_2$ interaction which makes the CuO reduction easier, as proposed in the case of highly dispersed CuO aggregates supported on titania (43). The reducibility of CuO, assessed from the temperature (T_m), where the reduction rate is maximum, decreases monotonously with the increase of sulfur content (Fig. 5). The H_2 uptake, H_2/Cu, which varies between 0.84 and 1.1 (Table 2) provides evidence that copper species are mainly reduced to Cu^0 before sulfate reduction becomes significant. In the TPR of Cu/SZ at constant sulfur content, the copper loading has a small effect on Cu species reducibility (Fig. 6). Nevertheless, the T_m was slightly shifted to a lower temperature by 35 K when copper loading increased. It should be pointed out that for Cu content lower than 1 wt%, it was difficult to quantify precisely the H_2 taken up by copper reduction due to superposition with the beginning of sulfate reduction. For each of these materials studied, the observed H_2/Cu ratio (Table 2), calculated from the TPR profile areas, shows that Cu species are mainly reduced to Cu^0 by 650 K, the temperature at which the first TPR experiment was carried out.

The TPO profiles, obtained after the first TPR run, are shown in Fig. 7. The TPO curves presented two oxidation peaks for all the catalysts studied. Oxygen taken up under the two peaks are very close whatever the sample; we may thus assume that reoxidation occurs in a two step process: $2\,Cu^0 + 1/2\,O_2 \rightarrow Cu_2O$, followed by $1/2\,Cu_2O + 1/2\,O_2 \rightarrow CuO$. The temperature T_{m2} at which the maximum rate of the re-oxidation process, $1/2\,Cu_2O + 1/2\,O_2 \rightarrow CuO$, occurs is shifted to higher values with the amount of sulfate contained in the catalyst. There was only a weak shift of T_{m1} and T_{m2} to higher temperature upon increasing the Cu content and, thus, a weak influence of Cu content on the oxidisability of Cu species (Table 2). It is worth noting that, upon the increase of the sulfate content, both the reducibility and

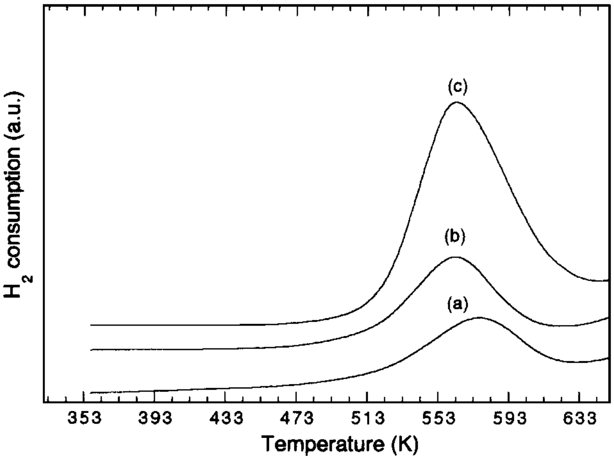

FIG. 6. TPR profiles of: (a) Cu(0.8)SZ(3.5); (b) Cu(3.9)SZ(3.5); and Cu(7.9)SZ(3.5). Conditions: H_2/Ar: 3/97 (vol/vol); flow rate = 20 cm^3 min^{-1}; amount of catalyst = 0.085 g; heating rate = 5 K min^{-1}.

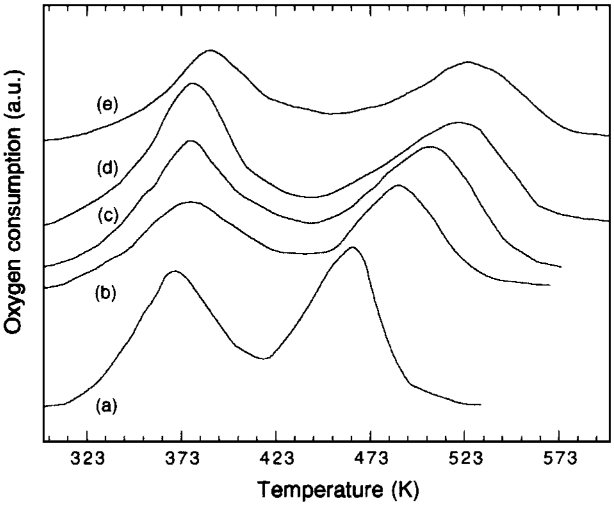

FIG. 7. TPO profiles of: (a) Cu(3.7)ZrO_2; (b) Cu(3.0)SZ(1.4); (c) Cu(4.0)SZ(2.5); (d) Cu(3.9)SZ(3.5); and (e) Cu(3.0)SZ(5.3). Conditions: O_2/He: 3/97 (vol/vol); flow rate = 20 cm^3 min^{-1}; heating rate = 5 K min^{-1}.

oxidisability of Cu species decreased. However, this effect is stronger on the reducibility, since the $Cu^{II} \rightarrow Cu^{0}$ step occurred at lower temperature than $Cu^{I} \rightarrow Cu^{II}$ on Cu/ZrO_2, but the reverse was true when the sulfur content exceeds 2 wt%.

A second TPR experiment was performed after the TPO. The resulting TPR profiles do not exhibit great differences in comparison with the first TPR profiles. Only a slight shift to T_m towards lower temperatures should be pointed out.

3.4 Catalytic Tests

In the SCR of NO by *n*-decane, at 70,000 h^{-1}, no activity was detected on ZrO_2 and SZ below 773 K. However, ZrO_2 promotes a weak NO conversion at higher temperatures. Two waves of NO conversion develop on Cu/ZrO_2 (Fig. 8): (i) the first around 563 K, where NO is selectively reduced to N_2, and (ii) the second at higher temperatures ($\approx$750 K), where NO is mainly oxidised to NO_2. In contrast, on Cu/SZ only NO_2 traces have been detected in the whole temperature range during the SCR of NO. It is known that the strength of acid sites developed by SZ depends on the calcination temperature and became maximum for a calcination around 923 K (25, 44). Actually, the calcination of Cu/SZ at temperatures higher than 773 K (i.e., 873 K) leads to (i) a catalyst with a loss by ca 20% in sulfur content and of copper accessibility by ca 40% and (ii) a catalyst less active in NO reduction (Fig. 8). From these results, a high temperature of calcination, while it enhances the strength of acid sites of the catalyst, is not beneficial for the SCR of NO. On the other hand, the increase of sulfate content favours the reduction of NO to N_2 in a wide range of temperatures (Fig. 9); moreover, the temperature where the conversion of NO is maximum is shifted to higher values (Fig. 9 and Table 3). The oxidation of *n*-decane which yields essentially CO_2, starts at ca 523 K, a temperature lower than the reduction of NO; trace amounts of CO were only detected at temperatures below 673 K. Moreover, the presence of sulfate slightly shifts this temperature by 20–30 K towards higher values. Table 3 reports the conversion of NO to N_2 at 573, 623, and 673 K for all the catalyst studied. It is clear that NO reduction is enhanced by sulfur content and reaches a

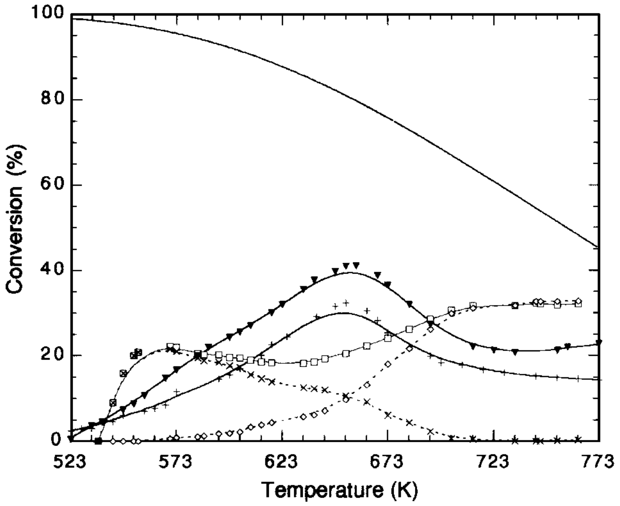

FIG. 8. NO conversion in the SCR of NO by *n*-decane on: (□) $Cu(3.7)ZrO_2$; (▼) Cu(4.0)/SZ(2.5) calcined at 773 K; (+) Cu(4.0)/SZ(2.5) calcined at 873 K; (×) NO conversion to N_2; and (◇) NO conversion to NO_2 on $Cu(3.7)ZrO_2$; (———) thermodynamic equilibrium $NO + 1/2\ O_2 \Leftrightarrow NO_2$ with 1000 ppm ($NO + NO_2$) and 9% O_2. Conditions: feed 1000 ppm NO; 0.03% *n*-decane; 9% O_2; balance with helium; flow rate = 60 $cm^3\ min^{-1}$; amount of catalyst = 0.050 g; heating rate = 5 K min^{-1}.

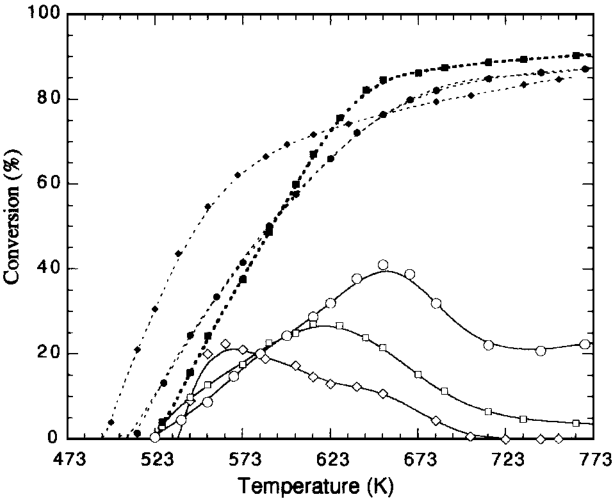

FIG. 9. Effect of the sulfur content in the SCR of NO by *n*-decane on Cu/SZ catalysts: (◇, ◆) $Cu(3.7)ZrO_2$, (□, ■) Cu(3.0)/SZ(1.0), and (○, ●) Cu(4.0)/SZ(2.5)NO; open symbols, conversion of NO to N_2; full symbols, *n*-decane conversion to CO_2. Conditions: feed 1000 ppm NO, 0.03% *n*-decane, 9% O_2, balance with helium, flow rate = 60 $cm^3\ min^{-1}$, amount of catalyst = 0.050 g, heating rate = 5 K min^{-1}.

TABLE 3

Some Catalytic Properties of the SCR of NO by *n*-Decane on Zirconia-Supported Catalysts

Catalysts	Conversion of NO to N_2 (%) 573 K	623 K	673 K	Maximum of NO conversion Temperature (K)	Conversion (%)
$Cu(3.7)/ZrO_2$	22	13	6	558	22
Cu(3.0)/SZ(1.0)	18	27	15	623	27
Cu(3.0)/SZ(1.4)	17	25	17	642	29
Cu(4.0)/SZ(2.5)	17	31	35	653	40
Cu(3.9)/SZ(3.5)	20	34	38	653	45
Cu(3.0)/SZ(5.3)	8	6	14	683	20
SZ(3.5)	0	0	0	—	—
Cu(0.8)/SZ(3.5)	0	3	7	738	28
Cu(3.2)/SZ(3.5)	13	26	33	655	38
Cu(7.9)/SZ(3.5)	12	28	18	634	38

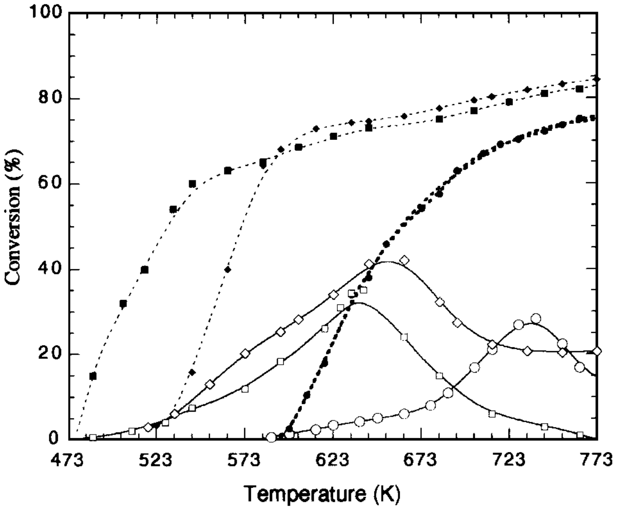

FIG. 10. Effect of copper content in the SCR of NO by *n*-decane on Cu/SZ catalysts: (○, ●) Cu(0.8)/SZ(3.5), (◇, ◆) Cu(3.9)/SZ(3.5), and (□, ■) Cu(7.9)/SZ(3.5); open symbols, conversion of NO to N_2; full symbols, *n*-decane conversion to CO_2. Conditions: feed 1000 ppm NO, 0.03% *n*-decane, 9% O_2, balance with helium, flow rate = 60 cm^3 min^{-1}, amount of catalyst = 0.050 g, heating rate = 5 K min^{-1}.

maximum value for a sulfate coverage close to the theoretical monolayer (3.5 wt%).

A Cu amount, deposited on SZ(3.5), as small as 0.8 wt% is sufficient to induce 10–30% reduction of NO to N_2 below 750 K (Fig. 10). The maximum of NO conversion is observed for Cu(3.2)/SZ(3.5) (Fig. 10). Both the temperature where the conversion of NO to N_2 is maximum, and the temperature at which hydrocarbon oxidation starts, decrease as the amount of copper increases.

4. DISCUSSION

At first, one should point out that the use of $Cu(acac)_2$, as precursor, and the protocol developed by Boitiaux *et al.* (22) for precursor deposition, have allowed the preparation of model Cu/SZ catalysts. In these catalysts, the Cu and sulfate contents have been thus monitored, in a wide range of composition, independently.

As expected, the doping of ZrO_2 by sulfate has improved the acidity of the solid. It was maximised, for both the number and strength of acid sites, at a S content near a theoretical monolayer of sulfate, i.e. 3–4 wt% S for 220 m^2 g^{-1}.

Whatever the catalyst, Cu species are under the form of CuO aggregates, as shown by UV-Vis and ESR spectroscopies, and TPR experiments. These aggregates exhibit a poorly organised structure, without any XRD diffraction line. This is even true for the Cu(7.9)SZ(3.5) sample in which the accessibility of Cu to NO was low, NO/Cu = 0.08 (39). It was actually concluded that the low accessibility, observed at high S content was due, in part, to the interaction of sulfates with Cu species onto the CuO aggregates (45).

Besides the decrease of accessibility in these CuO aggregates, the presence of sulfate lowers the reducibility of Cu species too. Upon addition of 5.3 wt% S, the temperature of faster reduction rate was shifted by 190 K to higher values. The sulfate species are likely interacting with the CuO surface and decrease the reducibility of Cu^{II} by an electron withdrawing effect. FTIR studies of NO adsorption on Cu/SZ have provided evidence of this effect (45). After adsorption of NO at room temperature, mononitrosyl Cu(NO) and nitrito are the main species occurring at the surface of CuO aggregates. In the presence of sulfate, only the Cu(NO) species remain and ν_{NO} is shifted from 1872 to 1910 cm^{-1}. This shift was accounted for a decrease of the electron density at the Cu^{II} sites due to the electron withdrawing effect of sulfate species. A similar explanation was proposed for the lower reducibility of Ni and Pt in Pt/SZ (39, 40). Finally, the presence of Cu shifted to lower temperatures the reduction onset of sulfate species.

The oxidation by 3% O_2 in He, of Cu^0 both in ZrO_2 and SZ proceeds in two steps; i.e. $Cu^0 \rightarrow Cu_2O$ then $Cu_2O \rightarrow CuO$. The lower oxidisability of Cu species, in the presence of sulfates, parallels that observed for the reducibility. Both steps of Cu oxidation are shifted by 40 and 70 K to higher temperatures, respectively. The TPO were performed on the samples after carrying out the TPR experiments. It is, therefore, likely that the Cu^0 aggregates are in interaction with both sulfate and some traces of sulfur species. The later being formed by reduction of some sulfate species, which began just before the end of the TPR runs. We may assume that patches of sulfates decorate the Cu^0 aggregate surface, making their oxidation more difficult.

$Cu(3.7)/ZrO_2$ is active and selective in NO reduction by *n*-decane up to 573 K with a maximum at 558 K. Above 573 K, NO_2 is detected and the catalyst become fully selective in NO_2 at 718 K with a conversion reaching 33%. On co-precipitated copper-zirconia oxide catalysts, Kung *et al.* (46) observed a maximum of conversion at 561 K in the SCR of NO by propene for a catalyst containing 6.0 wt% of copper. These authors explain the high reactivity and selectivity of low Cu loaded Cu–Zr–O mixed oxides by the high dispersion of copper on zirconia. A good accessibility was also observed for $Cu(3.7)/ZrO_2$ (Table 1). An assumption similar to that proposed by Kung *et al.* (46) can be put forward to explain the high NO reduction activity below 560 K, but it cannot explain the different behavior observed at higher temperature. These differences may be either due to the nature of the reductant or to the catalyst preparation.

The presulfation of zirconia leads to Cu/SZ catalyst fully selective in NO conversion to nitrogen in the whole range of temperatures. In Fig. 11, the turnover frequency (TOF) for NO reduction in N_2 (*conversions in Table 3*) expressed per accessible Cu site, determined by TPD of NO, has been

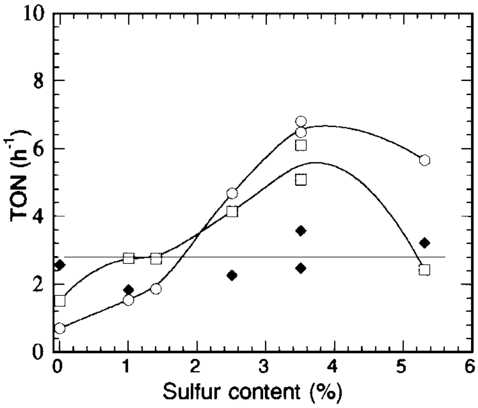

FIG. 11. Effect of the sulfur content on the TOF of the SCR of NO to N_2 by *n*-decane on Cu(3–4)/SZ(y) catalysts at: (◆) 573 K, (☐) 623 K, and (○) 673 K.

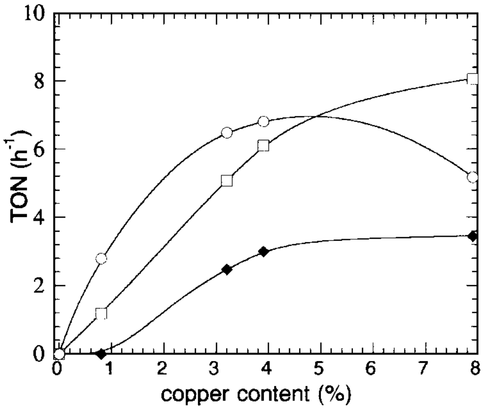

FIG. 12. Effect of copper content on the TOF of the SCR of NO to N_2 by *n*-decane on Cu(x)/SZ(3.5) catalysts at: (◆) 573 K, (☐) 623 K, and (○) 673 K.

reported at three temperatures, i.e. 573, 623, and 673 K, as a function of S content. At 573 K, the TOF remains close to 2.8 h^{-1} whatever the sulfur content. Therefore, this suggests that acidity does not play a significant role at 573 K. On the other hand, at 623 and 673 K, the TOF goes through a maximum at 3.5 wt% S and then decreases. Moreover, the highest values of TOF may be underevaluated due to some mass transfer limitations (NO conversions: 30–40%). Thus, a maximum of activity is reached with an amount of sulfur of ca 3.5% which corresponds to a sulfate coverage close to the theoretical monolayer. As expected, Cu(3.9)SZ(3.5) presents the greatest number and highest strength of acid sites among the Cu/SZ studied. Several authors (12, 47) have pointed out a correlation between the number of acid sites and the activity in the SCR of NO. On H-form zeolites, Satsuma *et al.* (12) thus correlate the activity of NO reduction by propene to the number of acid sites and a similar result was previously reported by Kintaichi *et al.* (47) on silica-alumina catalysts.

Cu-free SZ solids are inactive below 773 K whatever the amount of sulfur. On the other hand, the increase of copper content in Cu/SZ shifts to lower temperature the maximum of conversion and widens the conversion window. The TON, expressed per accessible Cu site, thus increases with copper amount up to 4 wt% then reaches a plateau (Fig. 12). This result shows that the presence of at least 4 wt% Cu is necessary to obtain the optimal combination between copper and sulfate species. It is often proposed that the SCR mechanism goes through the oxidation of NO to NO_2 in the first step followed by "nitration" of the activated hydrocarbon in a second step; the nitro-organic compound being then decomposed to N_2 and CO_2 through different surface intermediates (5, 48). The acid properties generated by impregnation of zirconia with sulfate must enhance sharply hydrocarbon nitration and therefore are essential to maintain the selectivity in N_2 above 600 K for Cu/SZ catalysts.

By using the same experimental conditions, the NO reduction profiles by *n*-decane on Cu/MFI and Cu(3.9)/SZ(3.5) are shown in Fig. 13. Cu(80)MFI is indeed more active but only in the 673–743 K temperature range. By contrast, Cu(3.9)/SZ(3.5) exhibits a much higher conversion between 520 to 650 K.

In conclusion, the adequate balance between the acid and redox functions of Cu/SZ, obtained through a dedicated preparation of Cu(3.9)/SZ(3.5), generates an efficient and selective catalyst in the SCR of NO by *n*-decane in the presence of oxygen. The maximum acidity was obtained by deposition of a sulfate amount close to that required to form a theoretical monolayer. In this catalyst, copper is

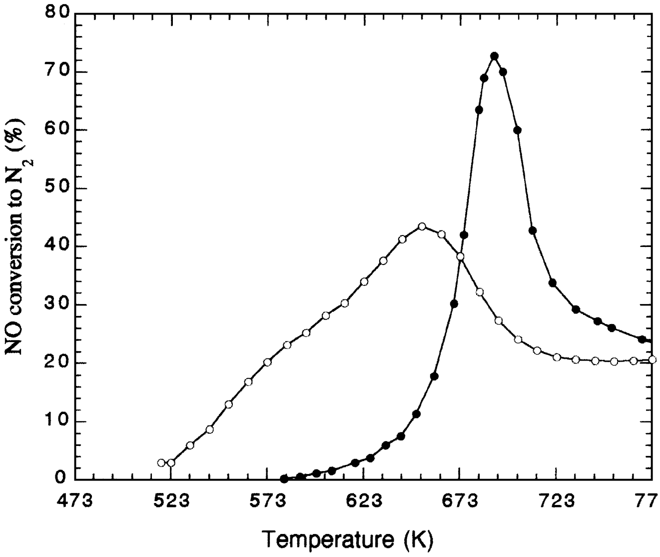

FIG. 13. NO conversion in the SCR of NO by *n*-decane on Cu/MFI (●) and Cu(3.9)/SZ(3.5) (○) catalysts. Conditions: feed 1000 ppm NO, 0.03% *n*-decane, 9% O_2, balance with helium, flow rate = 60 cm^3 min^{-1}, amount of catalyst = 0.050 g, heating rate = 5 K min^{-1}.

(i) in the form of well dispersed CuO aggregates and (ii) in strong interaction with sulfate species. Both the reducibility and oxidisability of Cu species decrease when sulfate content increases. The acidity plays thus a crucial role by maintaining a complete selectivity to N_2 in the whole range of temperature.

ACKNOWLEDGMENT

Support of this work by the European Union (BRITE EURAM II Contract BRE2-CT92-0192) is gratefully acknowledged.

REFERENCES

1. Amiridis, M. D., Zhang, T., and Farrauto, R. J., *Appl. Catal. B* **10**, 203 (1996).
2. Witzel, F., Sill, G. A., and Hall, W. K., *J. Catal.* **149**, 229 (1994).
3. Adams, K. M., Cavataio, J. V., and Hammerle, R. H., *Appl. Catal. B* **10**, 157 (1996).
4. Burch, R., and Millington, P. J., *Appl. Catal. B* **2**, 101 (1993).
5. Gaudin, C., Duprez, D., Mabilon, G., and Prigent, M., *J. Catal.* **160**, 10 (1996).
6. Petunchi, J. O., and Hall, W. K., *App. Catal. B* **2**, L17 (1993).
7. Chajar, Z., Primet, M., Praliaud, H., Chevrier, M., Gauthier, C., and Mathis, F., *Catal. Lett.* **28**, 33 (1994).
8. Sasaki, M., Hamada, H., Kintaichi, Y., and Ito, T., *Catal. Lett.* **15**, 297 (1992).
9. Delahay, G., Coq, B., Ensuque, E., and Figuéras, F., *Catal. Lett.* **39**, 105 (1996).
10. Delahay, G., Coq, B., Ensuque, E., and Figuéras, F., *C.R. Acad. Sci. II B* **322**, 881 (1996).
11. Figuéras, F., Coq. B., Mabilon, G., Prigent, M., and Tachon, D., *in* “Studies in Surface Science and Catalysis” (J. W. Hightower, W. N. Delgass, E. Iglesia, and A. T. Bell, Eds.), Vol. 101, p. 621. Elsevier, Amsterdam, 1996.
12. Satsuma, A., Yamada, K., Mori, T., Niwa, M., Hattori, T., and Murakami, Y., *Catal. Lett.* **31**, 367 (1995).
13. Hamada, H., Kintaichi, Y., Yoshinari, T., Tabata, M., Sasaki, M., and Ito, T., *Catal. Today* **17**, 111 (1993).
14. Loughran, C. J., and Resasco, D. E., *Appl. Catal. B* **7**, 113 (1995).
15. Yokoyama, C., and Misono, M., *Bull. Chem. Soc. Japan* **67**, 557 (1994).
16. Hamada, H., Kintaichi, Y., Tabata, M., Sasaki, M., and Ito, T., *Chem. Lett.*, 2179 (1991).
17. Inui, T., Iwamoto, S., Kojo, S., and Yoshida, T., *Catal. Lett.* **16**, 223 (1992).
18. Yogo, K., Umeno, M., Watanabe, H., and Kikuchi, E., *Catal. Lett.* **19**, 131 (1993).
19. Li, Y., and Armor, J. N., *J. Catal.* **145**, 1 (1994).
20. Hamada, H., Kintaichi, Y., Sasaki, M., Ito, T., and Tabata. M., *Appl. Catal.* **64**, L1 (1990).
21. Hamada, H., *Catal. Today* **22**, 21 (1994).
22. Boitiaux, J. P., Cosyns, J., and Vasudevan, S., *in* “Studies in Surface Science and Catalysis” (G. Poncelet, P. Grange, and P. A. Jacobs, Eds.), Vol. 16, p. 123. Elsevier, Amsterdam, 1982.
23. Figuéras, F., Coq, B., Walter, C., and Carriat, J. Y., *J. Catal.* **169**, 103. (1997).
24. Coq, B., Tachon, D., Figuéras, F., Mabilon, G., and Prigent, M., *Appl. Catal. B* **6**, 271 (1995).
25. Arata, K., *Adv. Catal.* **37**, 165 (1990).
26. Corma, A., Fornés, V., Juan-Rajadell, M. I., and López Nieto, J. M., *Appl. Catal. A* **116**, 151 (1994).
27. Nascimento, P., Akratopoulou, C., Oszagyan, M., Coudurier, G., Travers, C., Joly, J. F., and Vedrine, J. C., *in* “Proceedings of the 10th International Congress on Catalysis, Budapest (1992)” (L. Guzci, F. Solymosi, and P. Tetenyi, Eds.), Vol. B, p. 1185. Akadémiai Kiado, Budapest, 1993.
28. Armendariz, H., Coq, B., Tichit, D., Dutartre, R., and Figuèras, F., *J. Catal.*, in press.
29. Lavalley, J. C., *Catal. Today* **27**, 377 (1996).
30. Pelmenschikov, A. G., van Santen, R. A., Jänchen, J., and Meijer, E., *J. Phys. Chem.* **97**, 11071 (1993).
31. Kustov, L. M., Kazansky, V. B., Figuéras, F., and Tichit, D., *J. Catal.* **150**, 143 (1994).
32. Tanabe, K., *Mater Chem. Phys.* **13**, 347 (1985).
33. Bensitel, M., Saur, O., Lavalley, J. C., and Morrow, B. A., *Mater. Chem. Phys.* **19**, 147 (1988).
34. Morterra, C., Cerrato, G., and Bolis, V., *Catal. Today* **17**, 105 (1993).
35. Escalona Platero, E., and Peñarroya Mentruit, M., *Catal. Lett.* **30**, 31 (1995).
36. Jacobs, P. A., de Wilde, W., Schoonheydt, R. A., and Uytterhoeven, J. B., *J. Chem. Soc. Faraday Trans. I* **72**, 1221 (1976).
37. Shimokawabe, M., Asakawa, H., and Takezawa, N., *Appl. Catal.* **59**, 45 (1990).
38. Centi, G., Cerrato, G., d’Angelo, S., Finardi, U., Giamello, E., Morterra, C., and Perathoner, S., *Catal. Today* **27**, 265 (1996).
39. Coq, B., Walter, C., Brown, R., McDougall, G., and Figueras, F., *Catal. Lett.* **39**, 197 (1996).
40. Yori, J. C., and Parera, J. M., *Appl. Catal. A* **129**, 83 (1995).
41. Xu, B. Q., and Sachtler, W. M. H., *J. Catal.* **167**, 224 (1997).
42. Jones, A., and McNicol, B. D., *Chem. Ind.* **24**, 129 (1986).
43. Delk, F. S., and Vavere, A., *J. Catal.* **85**, 380 (1984).
44. Davis, B. H., Keogh, R. A., and Srinivasan, R., *Catal. Today* **20**, 219 (1994).
45. Delahay, G., Coq, B., Ensuque, E., Figuéras, F., Saussey, J., and Poignant, F., *Langmuir* **13**, 5588 (1997).
46. Kung, M. C., Bethke, K. A., and Kung, H. H., *in* “207th National Meeting ACS, San Diego, 1993” (S. K. Argawal and G. M. Marcelin, Eds.), p. 154.
47. Kintaichi, Y., Hamada, H., Tabata, M., Sasaki, M., and Ito, T., *Catal. Lett.* **6**, 239 (1990).
48. Adelman, B. J., Beutel, T., Lei, G.-D., and Sachtler, W. M. H., *Appl. Catal. B* **11**, L1 (1995).